Published in final edited form as:

Anal Chem. 2016 June 21; 88(12): 6492–6499. doi:10.1021/acs.analchem.6b01211.

Evaluation of Drug Concentrations Delivered by Microiontophoresis

Douglas C. Kirkpatrick[†] and **R. Mark Wightman**[†,‡,*]

[†]Department of Chemistry, University of North Carolina at Chapel Hill, Chapel Hill, North Carolina, 27599-3290, United States

[‡]Neuroscience Center, University of North Carolina at Chapel Hill, Chapel Hill, North Carolina, 27599-3290, United States

Abstract

Microiontophoresis uses an electric current to eject a drug solution from a glass capillary and is often utilized for targeted delivery in neurochemical investigations. The amount of drug ejected, and its effective concentration at the tip, has historically been difficult to determine, which has precluded its use in quantitative studies. To address this, a method called controlled iontophoresis was developed which employs a carbon-fiber microelectrode incorporated into a multibarreled iontophoretic probe to detect the ejection of electroactive species. Here, we evaluate the accuracy of this method. To do this, we eject different concentrations of quinpirole, a D2 receptor agonist, into a brain slice containing the dorsal striatum, a brain region with a high density of dopamine terminals. Local electrical stimulation was used to evoke dopamine release, and inhibitory actions of quinpirole on this release were examined. The amount of drug ejected was estimated by detection of a coejected electrochemical marker. Dose response curves generated in this manner were compared to curves generated by conventional perfusion of quinpirole through the slice. We find several experimental conditions must be optimized for accurate results. First, selection of a marker with an identical charge was necessary to mimic the ejection of the cationic agonist. Next, evoked responses were more precise following longer periods between the end of the ejection and stimulation. Lastly, the accuracy of concentration evaluations was improved by longer ejections. Incorporation of these factors into existing protocols allows for greater certainty of concentrations delivered by controlled iontophoresis.

Graphical abstract

[*]Corresponding Author: rmw@unc.edu. Phone: (919) 962-1472.

Author Contributions

All authors have given approval to the final version of the manuscript.

The authors declare no competing financial interest.

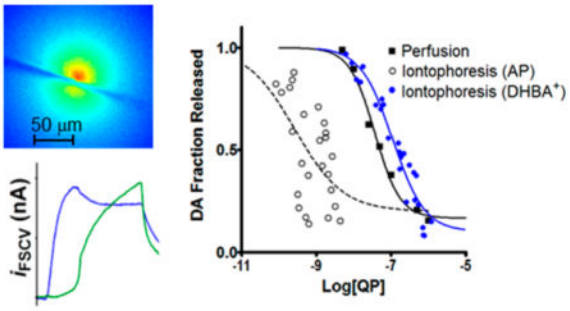

Microiontophoresis is the ejection of solute from a capillary by an electric current. This technique has been widely used in neuroscience to deliver agents to specific areas of the brain.[1–4] While offering advantages over conventional delivery methods, the inability to determine ejection quantity or confirm drug delivery has impeded micro-iontophoresis from having greater impact. Indeed, the modern use of microiontophoresis is primarily for qualitative investigations.[5–9] Commonly, the ejection quantity is varied by adjusting the magnitude of the ejection current, but such methods are usually carried out without confirmation of the delivered amount.[10–12] Because similar ejection conditions can result in different delivery rates, most users do not make precise claims of their ejection concentrations.

Theoretical attempts to determine ejection quantities have assigned transport numbers to specific analytes.[13] However, slight variations in barrel geometries cause different transport numbers between similarly fabricated probes.[14] Additionally, the ejection medium may influence the concentration distribution, rendering estimates of concentration from the ejection quantity meaningless.[15,16] Measurement strategies for ejected solutions have shown more promise, as electrodes positioned near or adjacent to the barrel can detect the delivery of electroactive substances, as can fluorescence measurements for fluorophores, without affecting delivery to the adjacent region.[17–21] These methods have the advantage of providing simultaneous information regarding the ejection progress with locally collected physiological data.[22–24] One technique for monitoring ejections, controlled iontophoresis, employs a carbon-fiber microelectrode incorporated into a multibarreled probe, with the remaining barrels used for ejections.[25,26] Ejection of an electroactive substance can be detected and quantified, and its concentration is related to that of a coejected inactive compound if the relative mobilities are known.[27] For use in brain tissue, the electroactive species, or marker, must be inert to the neurochemical processes under investigation.[28]

We have previously shown that ejection rates of markers and drugs are consistent and can be determined from their mobilities in capillary electrophoresis because the same mass transport mechanisms, electroosmotic flow and migration, are operant in both techniques.[29] In this study, ejections of quinpirole (QP), a D2 receptor agonist, were performed with an electrochemical marker to estimate the drug delivery quantity. QP inhibits dopamine (DA) release in a dose-dependent manner by binding to the autoreceptor on presynaptic DA terminals.[30] Using the diminished stimulated DA release quantity following QP ejections and the electrochemical signal from the marker, we determined the accuracy of calculated

ejected drug concentrations. Our initial results had large discrepancies between the calculated concentrations and the observed effects. We then determined the causes of the poor predictions by evaluating the factors that govern evaluations of ejected concentrations. Through this, it is shown how optimized methods can improve assessments of drug concentrations in controlled iontophoresis.

EXPERIMENTAL SECTION

Chemicals and Solutions

All chemicals were received from Sigma-Aldrich (St. Louis, MO). Artificial cerebral spinal fluid (aCSF) consisted of 126 mM NaCl, 2.5 mM KCl, 1 mM NaH_2PO_4, 26 mM $NaHCO_3$, 2 mM $MgSO_4$, 2 mM $CaCl_2$, and 11 mM glucose and adjusted to pH 7.4. Iontophoretic solutions were made fresh daily from deionized water, and the pH was consistently measured between 6 and 7. To prevent clogging, solutions were filtered (0.45 μm Nylon, Nalgene, USA) before addition to the barrel.

Iontophoresis with Fast-Scan Cyclic Voltammetry

Four-barreled iontophoresis probes (0.5–1 μm tip diameter) were fabricated from prefused glass capillaries (Friedrich & Dimmock, Millville, NJ) as previously described.[27] One of the barrels held a capillary containing a carbon fiber (7 μm diameter) cut to approximately 100 μm while the other barrels were available for ejections. A homemade current source (UNC Electronics Facility, Chapel Hill, NC) was used in combination with customized LabVIEW code (National Instruments, Austin, TX) to control ejections through an NI-USB-6343 DAQ card (National Instruments). For each ejection, a constant current was applied to the barrel and the corresponding voltage data was recorded. A single Ag/AgCl reference electrode (World Prescision Instruments, Sarasota, FL) held at ground potential was used as the return for iontophoretic ejections and for voltammetry experiments.

As the ejection proceeded, ejected electroactive species were detected by fast-scan cyclic voltammetry (FSCV) at the carbon-fiber microelectrode using a locally constructed instrument (UNC Chemistry Electronics Facility). HDCV software was used to control the potential during voltammetry and to collect data.[24] For detection of 2-(4-nitrophenoxy) ethanol (NPE) with DA or acetaminophen (AP), waveform parameters were chosen so that each species could be resolved.[29] The waveform began from a −0.7 V holding potential, was scanned to −1.3 V, then to 1.0 V, and finally returned to the holding potential. This was done at a scan rate of 200 V/s and repeated at 10 Hz. For dose–response experiments, a waveform was used which optimized the DA signal.[31] This utilized a holding potential of −0.4 V, which was then scanned to an upper limit of 1.0 V before returning to the holding potential. The scan rate was 600 V/s, and the waveform was repeated at 10 Hz. All voltammograms underwent digital background subtraction, averaging, and filtering (2–10 kHz) prior to analysis.[24]

Fluorescence Microscopy

Iontophoretic barrels were filled with a 10 mM tris(2,2′-bipyridyl)dichlororuthenium(II) ($Ru(bpy)_3Cl_2$) and 5 mM NaCl solution. A micromanipulator (MPC-200-ROE, Sutter

Instruments, Novato, CA) was used to insert the barrel tip ~50 μm beneath the surface of a 1% agarose block made from aCSF, which was positioned in a holding chamber on the stage of an Eclipse FN1 microscope (Nikon Instruments). Additional aCSF was added around the agarose in which the Ag/AgCl reference electrode was placed. The microscope was equipped with a xenon halide illumination source (X-Cite 120, EXFO), and filter cubes were used to select the excitation (450–490 nm) and emission (500–550 nm) wavelengths. Images were captured with a Retiga Exi camera (QImaging, Surrey, BC, Canada) at a resolution of 1 pixel/μm and recorded with QCapture software (QImaging).

Ejections of $Ru(bpy)_3Cl_2$ (120 nA) were performed for 5, 15, or 60 s, and images were recorded every 3–10 s. Additional images were recorded for 1 min following ejection termination. A Matlab script (Mathworks, Natick, MA) was used to determine the average radial $Ru(bpy)_3^{2+}$ distribution of each image by averaging the fluorescence intensity along 11 background subtracted cross-sectional lines spanning from the barrel tip.[32]

Animal Care and Use

Sprague–Dawley male rats (250–350 g, Charles River, Wilmington, MA) were used for all *in vitro* experiments. Prior to use, rats were dually housed and provided with food and water *ad libitum*. Procedures were approved by the Institutional Animal Care and Use Committee at the University of North Carolina at Chapel Hill. Special care was taken to limit the number of animals used and to reduce their suffering.

Brain Slice Preparation

Following urethane (1.5 g/kg) anesthesia, brains were quickly removed and placed in chilled oxygenated (95/5% O_2/CO_2) aCSF. A vibratome (VF-200, Precisionary Instruments, San Jose, CA) equipped with a stainless steel feather blade (Fendrihan, USA) was used to cut 300 μm thick coronal slices containing the anterior dorsal striatum. After cutting, slices were allowed to recover for at least 1 h in 20 °C aCSF. For recordings, slices were anchored (SHD-22KIT, Warner Instruments, Hamden, CT) in a perfusion chamber (RC-22, Warner Instruments) on the microscope stage. A continuous (2 mL/min) stream of 37 °C oxygenated aCSF was perfused through the chamber. A 30 min equilibration period in the perfusion chamber was assigned for each slice prior to measurements.

Dose–Response Curves

A bipolar tungsten electrode with 250 μm spacing (MicroProbes, Gaithersburg, MD) was used to evoke DA release. It was inserted ~50 μm below the surface of a brain slice in the dorsal striatum. Release was evoked by a single 350 μA biphasic pulse (2 ms/phase) and detected using FSCV at a carbon-fiber microelectrode positioned midway between the stimulating electrodes. To avoid electrical interference, the stimulation was applied 10 ms before the FSCV waveform. Release was evoked at 4 min intervals. After an initial conditioning phase of approximately 30 min, DA release was stable, changing by less than 10% between stimulations.[30,33] To apply QP via perfusion, the standard aCSF stream was switched to aCSF containing a known concentration of the drug. Stimulation continued every 4 min until released DA stabilized at a new concentration, typically achieved within 20–30 min.[34] This value was taken as the effect of the drug and was compared to predrug

release. Dosages were applied in increasing order, with no more than four concentrations per slice.

For iontophoretic experiments, the carbon-fiber micro-electrode was incorporated in a multibarreled probe, positioned in the dorsal striatum at a location similar to those in the perfusion experiments. Identical biphasic electrical stimulations were used, and coejections (5, 15, or 60 s) of QP and an electrochemical marker were performed after consistent DA release was established. Stimulation occurred at precise times after the ejection (3, 15, or 60 s). The amount of DA released from stimulation after the ejection was recorded as the postdrug release quantity. Ejections were timed so that a 4 min stimulation rate was maintained. To allow recovery from previous administration, two stimulations were performed between successive ejections. AP and DHBA were used independently as markers to monitor ejections via oxidation on the carbon-fiber electrode. For AP trials, a 1 mM solution of the marker, 0.3 μM QP, and 5 mM NaCl was ejected. For DHBA, the concentrations of the marker, QP, and NaCl were chosen on the basis of the ejection duration and time before stimulation to allow for complete coverage of the dose–response curve and to ensure for detection of the marker within the linear calibration range. Exact barrel concentrations are reported individually for each case.

Statistical Analysis of Dose–Response Data

Regression curves and parameters for dose–response data were determined in Prism (GraphPad Software, La Jolla, CA) using a sigmoidal dose–response (variable slope) model, which employs a four parameter logistic Hill equation to fit data. Constraints were applied for the maximum equal to 1.0 and the bottom less than or equal to 0.2. These were required for several iontophoresis data sets (AP and DHBA with 3 s wait time) which displayed highly varied responses and were chosen on the basis of perfusion results. All p-values reported for the best-fit parameters were calculated using the comparison method with an F test.

RESULTS AND DISCUSSION

Advantages of Microiontophoretic Drug Delivery

Quantitative drug application is challenging in neurochemical investigations. Doses administered *in vivo* are typically based on the animal's mass, but uptake and metabolism ultimately determine the effective concentration at the region of interest. *In vitro* experiments can more reliably perfuse known concentrations throughout a brain slice, but long application times are required to attain equilibrium. The perfusion procedure we employed is illustrated in Figure 1A. A carbon-fiber microelectrode was used to detect DA by FSCV in the dorsal striatum of a rat brain slice. The DA signal increased directly following electrical stimulation and returned to baseline shortly after. Failure to return to the exact baseline could be due to chemical interferences or electrode drift.[35] After the predrug release stabilized, 30 nM QP was administered. Evoked DA release gradually decreased during perfusion until a new stable release quantity was achieved. Due to the time required for the drug to diffuse into the slice, its full inhibitory effect was not realized until nearly 20 min after its application.

In contrast, locally delivered drugs from microiontophoresis take effect in seconds which allows for more rapid investigations. To illustrate this, Figure 1B shows a controlled iontophoresis ejection in which the oxidation current of a coejected marker, DHBA, was monitored by FSCV on a carbon-fiber microelectrode during QP delivery. The inhibitory effect of QP on stimulated DA release was observed 15 s after the ejection (Figure 1C).

Concentration Evaluations of Controlled Ejections

To determine concentrations of ejected species from controlled iontophoresis, eq 1 was used where i_m is the marker current at the end of the ejection, A_m is a flow-analysis calibration factor, $[M]_b$ and $[D]_b$ are the respective marker and drug barrel concentrations, $\frac{v_D}{v_M}$ is their mobility ratio in an electric field, and DF is a dilution factor.[28]

$$[D] = i_m \times A_m \times \frac{[M]_b}{[D]_b} \times \frac{v_D}{v_M} \times DF \quad (1)$$

The marker current, calibration factor, barrel concentrations, and electric mobility ratio provide the average concentration of the marker at the end of the ejection. The dilution factor adjusts for the amount of drug remaining at the time of stimulation, typically 5–120 s after the ejection is terminated. This value is empirically determined by the fraction of the marker oxidation current at the stimulation time compared to its steady-state value (Figure 1B). The ability of eq 1 to yield ejection concentrations was tested by comparing responses of controlled iontophoresis to those obtained from perfusion of QP, the standard drug delivery method for slice experiments. For perfusion, known QP concentrations were administered to the slice and the electrically evoked DA response was recorded after a new stable value was obtained. This quantity was compared to the predrug release amount, and as indicated by the error bars, results were highly reproducible (Figure 2, squares). Best-fit parameters from a four parameter Hill regression model yielded an IC_{50}, the drug concentration which inhibits maximal release by half, of 37 nM, a Hill slope, indicating the cooperativity at the binding site, of −1.28 (Table 1), and a reasonable value of the correlation coefficient.[36] Each of these parameters agrees with previously reported values.[37,38] Next, dose–response data were collected for controlled iontophoretic delivery of QP, a monocation at the pH values employed. In these initial experiments, AP, a neutral molecule, was used as the electroactive marker. Ejections were 15 s in length, and DA release was evoked 15 s after the end of the ejection, with data obtained from 5 different iontophoretic probes due to barrel to barrel ejection variability.[39] Figure 2 (circles) shows the DA response to iontophoretic delivery of QP using eq 1 to evaluate ejection concentrations. These data have two major differences compared to the perfusion data. First, as reflected by the low correlation coefficient, the data were highly scattered and displayed a considerable degree of variance. Second, concentration estimates systematically underestimated the effective value, as a significantly different IC_{50} ($P < 0.0001$) was determined between delivery modes. Thus, controlled iontophoresis failed to produce either accuracy or precision in evaluation of ejected concentrations.

Initial Ejection Behavior Influenced by Molecular Charge

To understand the failure of eq 1 to reliably predict concentrations, the behavior of coejected species was further examined by ejecting a solution of DA, a protonated monocation at physiological pH, and the neutral molecule NPE into aCSF. These two compounds can be individually detected by FSCV during their coejection. Since mass transport in iontophoresis is a consequence of electroosmotic flow (EOF) and migration, ejection rates are dependent upon molecular charge and size.[29,40,41] Because these molecules are similarly sized, variation in their transport is primarily due to their charge difference, with EOF acting equally on both molecules while only DA is affected by migration. Temporal ejection profiles revealed a clear delay in NPE ejection compared to DA (Figure 3A). This indicates that initiation of mass transport by EOF lags that of migration.

The delayed action of EOF is due to the time required to eject the interfacial layer from the barrel tip. The interfacial layer is a heterogeneous region created by exchange between the barrel solution and the ejection medium during the time between ejections.[42] When the ejection was initiated, the voltage increased stepwise and rose more gradually as time progressed (Figure 3B). More voltage was required to maintain a constant ejection current because the highly ionic interfacial layer in the barrel tip was first ejected, increasing the total resistance of the barrel solution. Once this layer was cleared, the voltage approached steady state, and EOF was initiated.

Ejection Current Affects Interfacial Layer Clearance Time

To further characterize combined delivery, the experiment was repeated using different ejection currents that followed 3 min waiting periods. Differences in the ejected quantities of DA and NPE were more apparent at lower ejection currents (Figure 4A, upper). Further, the ratio of the faradaic current between the two species at the end of the ejections was dependent on the ejection current (Figure 4B, upper, ANOVA, $p = 0.0016$). This is because larger currents more quickly cleared the interfacial layer from the tip, which afterward allowed for the ejection of bulk barrel solution. For weaker ejections, the interfacial layer took longer to eject and, in some instances, was not cleared.

The problem of differential ejection rates was remedied by ejecting species of similar charge (Figure 4A, lower). When DA was replaced with AP, ejected quantities of the two neutral species were similar regardless of the ejection current (Figure 4B, lower, ANOVA, $p = 0.090$). These experiments explain why the neutral AP marker failed to reliably track the ejection of positively charged QP in the controlled iontophoresis dose–response experiment. Delayed EOF at the onset of ejections resulted in the delivery of the drug without the marker, leading to inconsistent and underestimated concentrations. Although we have previously documented significant EOF in barrels of high ionic strength (200 mM), these measurements were made for ejections lasting multiple minutes from barrels which were fully primed beforehand.[43] Continuous ejections of this sort prohibit the formation of an interfacial layer and, indeed, are often employed specifically for this purpose.[44,45] Additional work comparing DA and NPE ejection rates involved rapidly alternating between ejection and rest periods, conditions which similarly minimize the interfacial layer.[29] The key difference in the current study is that an interfacial layer was allowed to form during a 3

min waiting period prior to ejections, which caused the delay in EOF. Thus, the electric mobility term of eq 1 $\left(\frac{v_D}{v_M}\right)$ correcting for different ejection rates between dissimilarly charged species is dependent on the time required to eject the interfacial layer. However, as demonstrated, this term can be disregarded when the charge and molecular size of ejected species are similar because analytes of comparable mobility exhibit similar ejection behavior.

Reevaluating Ejection Concentrations with Modified Approaches

To further examine the failure of eq 1 to properly evaluate concentrations from controlled iontophoresis, the solute distribution of ejections was studied using fluorescence microscopy. $Ru(bpy)_3^{2+}$, a cationic fluorophore, was ejected into a 1% agarose gel which produces a similar distribution as ejections in brain tissue.[32] A color plot of the fluorescence intensity after 15 s of continuous ejection is shown in Figure 5A, which demonstrates how the maximum intensity occurs at the barrel tip and decays with spherical symmetry. Following a 15 s period with the ejection current turned off, the same distribution becomes much more uniform (Figure 5B). The time-course of the intensity at different locations during and following 15 s ejections is shown in Figure 5C. Due to the symmetrical nature of the distribution, these intensities represent the concentration on a sphere of radius r around the ejection point. Reduced concentrations after the ejection show the importance of the dilution factor (DF) in eq 1, which to this point was determined by the ratio of the marker current at stimulation compared to the steady state value. However, due to solute adsorption, concentration heterogeneity, and capacitive drift of the electrode, we feared this method was susceptible to error.[46] Instead, DF was determined from the fluorescence data. Figure 5D shows the average fluorescence intensity as a function of distance along the carbon fiber at the end of 15 s ejections and again for various waiting periods after the ejection was terminated. Each profile was integrated over a sphere to reveal the total amount of solute present. The ratio of the quantity after the waiting period compared to that at the end of the ejection gave the new fraction for DF. This value for the 15 s waiting period, 0.55, was larger than that obtained using the electrochemical estimate, 0.14, which resulted in the underestimated concentrations.

To study the ability of controlled iontophoresis to determine ejection concentrations with the updated dilution and mobility factor corrections, dose–response data were obtained for QP using DHBA as the electrochemical marker. Like QP, DHBA is a monocation, but it is electroactive and was found not to affect DA release in the striatum. Figure 6A shows that, unlike the results obtained with AP as the electroactive marker (Figure 2), evaluations using DHBA had a good correlation across multiple barrels and ejection current magnitudes (r^2 = 0.887). Thus, the imprecision of the data in Figure 2 was greatly improved by the use of a marker with an identical charge as the drug. However, neither this nor the new method for DF resolved the issue of inaccuracy, as the IC_{50} was overestimated by more than an order of magnitude (Table 2).

Drug Dilution to a Uniform Distribution Improves Precision

The waiting period between the end of the ejection and stimulation was next examined to determine its role on concentration evaluations. Dose–response data were generated using 15 s ejections with DHBA as the marker for waiting periods of 3 and 60 s (Figure 6B). The difference between IC_{50} values was insignificant, indicating that the duration of the waiting period did not affect accuracy (Table 2, $p = 0.774$). However, data for the 3 s waiting period were more weakly correlated compared to 15 and 60 s intervals. Thus, we concluded that an insufficient waiting period before stimulation can decrease precision, which could be due to several factors. First, shorter waiting periods result in a less uniform concentration across the electrode at the time of stimulation (Figure 5D). Terminals with D2 receptors are densely populated, and released DA diffuses only a few micrometers in the extracellular space before its uptake back into neurons.[47,48] This means that homogeneous DA release across the electrode necessitates a uniform drug concentration along the length of the carbon fiber, which can only be achieved with longer waiting periods. Second, the drug concentration around the electrode is less variable with longer times (Figure 5C). The half-life for dissociation of QP to D2 receptors is ~0.15 s,[49,50] so waiting periods spanning multiple half-lives allow more time for the drug and receptor to equilibrate at diluted concentrations. Interestingly, dilution to a nearly uniform and stable conformation occurs relatively quickly once ejections are terminated.

This is because the highest concentrated region accounts for only a fraction of the solute delivered during the ejection. Indeed, spherical integration of the fluorescence data for the 0 s profile in Figure 5D reveals that just 0.3% of ejected species are within 10 μm of the ejection origin, while more than 77% is located outside of 50 μm. Due to the spherical nature of the distribution, by which the volume increases with the third power of the radius, regions further away contain the majority of drug and more strongly influence the concentration upon dilution. Thus, a moderate wait time (15 s) after ejections is sufficient to form a more homogeneous concentration along the electrode.

Ejection Time Affects Accuracy of Concentration Evaluations

The effect of the ejection time was next examined by comparing QP dose–response data for 5 and 60 s ejections. Delivery was monitored with DHBA and DA stimulation occurred following a 15 s waiting period. Concentration evaluations grew more accurate with longer ejection times, and the IC_{50} better matched the perfusion standard (Figure 7A, Table 3). To determine why this occurred, the solute distribution for each duration was examined using fluorescence microscopy. As shown in Figure 7B, both ejections resulted in a concentration gradient along the electrode. These gradients are problematic because the average concentration of the ejection bolus, which the marker current is intended to represent, does not equal the average concentration along the electrode, which the marker current actually measures. Again, this is explained by the spherical distribution of ejected species, whose volume is not appropriately weighted by the marker current. For example, according to the 5 s profile, 25% of the marker current is produced within the first 10 μm of the electrode, despite this region containing just 0.5% of the total ejected species. Thus, smaller, more concentrated centers of spherical distributions disproportionately contribute to the marker current, leading to overestimated values of the average concentration.

Longer ejection durations resulted in more accurate IC_{50} values because they had less severe concentration gradients at the end of ejections. Since regions further from the origin become more concentrated with time, they are better represented by the concentration near the ejection point that dominates the marker signal. However, even the IC_{50} for the 60 s ejections significantly differed from that of perfusion ($p < 0.0001$), which we attribute to several factors. First, after 60 s of continuous delivery, the ejection concentration profile was still nonuniform along the electrode. Ideally, the distribution would be homogeneous to match the flow-injection analysis calibration conditions, but this is not achievable using extended ejections.[43] Second, biofouling on the surface of untreated carbon-fiber electrodes reduces sensitivity.[51,52] In fact, calibration following a 45 min incubation period in a slice revealed a decreased response of up to 80% in the current study. Lastly, some receptors may desensitize with prolonged exposure to drug, resulting in unreliable responses at the time of stimulation. However, this was unlikely the case in the current study, as D2 receptors are resilient to persistent exposure of QP.[53–55]

Even when optimized, there exists more quantitative uncertainty in concentrations determined from controlled iontophoresis than perfusion. However, in certain circumstances, the benefits of iontophoresis could well be worth this small sacrifice. This is because drugs can be administered more quickly by iontophoresis, with the combined ejection and waiting period lasting only 85 s for the most accurate parameter set (Figure 7A). In contrast, drugs delivered by perfusion require 10–20 min before their full effect is observed. Not only does faster administration increase throughput, but also it preserves slice health and receptor sensitization which are susceptible to prolonged application periods. Ultimately, the choice of a delivery method will depend upon the demands of the application, but as shown, controlled iontophoresis can provide a reliable drug delivery alternative for neurochemical investigations.

CONCLUSIONS

We have demonstrated methods to improve the accuracy and precision of concentration evaluations in controlled iontophoresis. To decrease uncertainty in the ejection status of a drug, markers should be used which share a similar molecular size and charge. For greater consistency in evoked responses, a moderate 15 s waiting period between the end of the ejection and stimulation allows the drug concentration to become more uniform. Finally, longer ejection times increase the accuracy of evaluations by decreasing the concentration gradient along the electrode. While concentration evaluations determined from controlled iontophoresis are still imperfect, these improvements, coupled with the benefits of highly localized application, offer advantages for investigations of drug effects.

Acknowledgments

The UNC Department of Chemistry Electronics Facility constructed the electrochemical and iontophoretic instruments. Research was funded by the NIH (DA010900).

References

1. Kovács P, Dénes V, Kellényi L, Hernádi I. J Pharmacol Toxicol Methods. 2005; 51:147–151. [PubMed: 15767208]
2. Staak R, Pape HC. J Neurosci. 2001; 21:1378–1384. [PubMed: 11160409]
3. Ni Z, Gao D, Bouali-Benazzouz R, Benabid AL, Benazzouz A. Eur J Neurosci. 2001; 14:373–381. [PubMed: 11553287]
4. Beckstead MJ, Grandy DK, Wickman K, Williams JT. Neuron. 2004; 42:939–946. [PubMed: 15207238]
5. Ayala YA, Malmierca MS. J Neurosci. 2015; 35:12261–12272. [PubMed: 26338336]
6. Patel CR, Zhang H. Front Neurol. 2014; 5:235. [PubMed: 25452744]
7. Leiras R, Velo P, Martín-Cora F, Canedo A. J Neurosci. 2010; 30:15383–15399. [PubMed: 21084595]
8. Wang T, Rusu SI, Hruskova B, Turecek R, Borst JGG. J Physiol. 2013; 591:4877–4894. [PubMed: 23940376]
9. Herr NR, Wightman RM. Front Biosci, Elite Ed. 2013; E5:249–257.
10. Bronzi D, Licata F, Li Volsi G. Neuroscience. 2015; 300:360–369. [PubMed: 26012489]
11. Lipski WJ, Grace AA. Neuropsychopharmacology. 2013; 38:285–292. [PubMed: 23032074]
12. Invernizzi RW, Pierucci M, Calcagno E, Di Giovanni G, Di Matteo V, Benigno A, Esposito E. Neuroscience. 2007; 144:1523–1535. [PubMed: 17161544]
13. Purves R. J Physiol. 1980; 300:72–73.
14. Bloom FE. Life Sci. 1974; 14:1819–1834. [PubMed: 4368008]
15. Trubatch J, Van Harreveld A. J Theor Biol. 1972; 36:355–366. [PubMed: 5073923]
16. Guy Y, Faraji AH, Gavigan CA, Strein TG, Weber SG. Anal Chem. 2012; 84:2179–2187. [PubMed: 22264102]
17. Ford CP, Gantz SC, Phillips PEM, Williams JT. J Neurosci. 2010; 30:6975–6983. [PubMed: 20484639]
18. Dionne VE, Steinbach JH, Stevens CF. J Physiol. 1978; 281:421–444. [PubMed: 309004]
19. Kaur G, Hrabetova S, Guilfoyle DN, Nicholson C, Hrabe J. J Neurosci Methods. 2008; 171:218–225. [PubMed: 18466980]
20. Inagaki K, Heiney SA, Blazquez PM. J Neurosci Methods. 2009; 178:255–262. [PubMed: 19135083]
21. Havey DC, Caspary DM. Electroencephalogr Clin Neurophysiol. 1980; 48:249–251. [PubMed: 6153344]
22. Haidarliu S, Shulz D, Ahissar E. J Neurosci Methods. 1995; 56:125–131. [PubMed: 7752678]
23. Kruk ZL, Armstrong-James M, Millar J. Life Sci. 1980; 27:2093–2098. [PubMed: 7207009]
24. Bucher ES, Brooks K, Verber MD, Keithley RB, Owesson-White C, Carroll S, Takmakov P, McKinney CJ, Wightman RM. Anal Chem. 2013; 85:10344–10353. [PubMed: 24083898]
25. Armstrong-James M, Millar J. J Neurosci Methods. 1979; 1:279–287. [PubMed: 544972]
26. Fu J, Lorden JF. J Neurosci Methods. 1996; 68:247–251. [PubMed: 8912197]
27. Belle AM, Owesson-White C, Herr NR, Carelli RM, Wightman RM. ACS Chem Neurosci. 2013; 4:761–771. [PubMed: 23480099]
28. Herr NR, Daniel KB, Belle AM, Carelli RM, Wightman RM. ACS Chem Neurosci. 2010; 1:627–638. [PubMed: 21060714]
29. Herr NR, Kile BM, Carelli RM, Wightman RM. Anal Chem. 2008; 80:8635–8641. [PubMed: 18947198]
30. Kennedy RT, Jones SR, Wightman RM. J Neurochem. 1992; 59:449–455. [PubMed: 1352798]
31. Heien MLAV, Phillips PEM, Stuber GD, Seipel AT, Wightman RM. Analyst. 2003; 128:1413–1419. [PubMed: 14737224]
32. Kirkpatrick DC, Edwards MA, Flowers PA, Wightman RM. Anal Chem. 2014; 86:9909–9916. [PubMed: 25157675]

33. Limberger N, Trout SJ, Kruk ZL, Starke K. Naunyn-Schmiedeberg's Arch Pharmacol. 1991; 344:623–629. [PubMed: 1775195]
34. Jones SR, Garris P, Wightman RM. J Pharmacol Exp Ther. 1995; 274:396–403. [PubMed: 7616424]
35. Schultz W, Carelli RM, Wightman RM. Current Opinion in Behavioral Sciences. 2015; 5:147–154. [PubMed: 26719853]
36. Khinkis LA, Levasseur L, Faessel H, Greco WR. Nonlinearity Biol, Toxicol, Med. 2003; 1:363–377. [PubMed: 19330140]
37. Miller, C. Improving Brain Slice Methodology. University of North Carolina, Chapel Hill; Chapel Hill, NC: 2008.
38. O'Neill C, Evers-Donnelly A, Nicholson D, O'Boyle KM, O'Connor JJ. J Neurochem. 2009; 108:545–551. [PubMed: 19187091]
39. Purves R. Trends Neurosci. 1980; 3:245–247.
40. Mudry B, Carrupt PA, Guy RH, Delgado-Charro MB. J Controlled Release. 2007; 122:165–172.
41. Mudry B, Guy RH, Delgado-Charro MB. Biophys J. 2006; 90:2822–2830. [PubMed: 16443654]
42. Bradshaw CM, Szabadi E. Neuropharmacology. 1974; 13:407–415. [PubMed: 4422089]
43. Kirkpatrick DC, Walton LR, Edwards MA, Wightman RM. Analyst. 2016; 141:1930. [PubMed: 26890395]
44. Rice ME, Nicholson C. J Neurophysiol. 1991; 65:264–272. [PubMed: 2016641]
45. Rice ME, Okada YC, Nicholson C. J Neurophysiol. 1993; 70:2035–2044. [PubMed: 7507522]
46. Johnson JA, Rodeberg NT, Wightman RM. ACS Chem Neurosci. 2016; 7:349. [PubMed: 26758246]
47. Venton BJ, Zhang H, Garris PA, Phillips PEM, Sulzer D, Wightman RM. J Neurochem. 2003; 87:1284–1295. [PubMed: 14622108]
48. Garris P, Ciolkowski E, Pastore P, Wightman R. J Neurosci. 1994; 14:6084–6093. [PubMed: 7931564]
49. Lepiku M, Rinken A, Järv J, Fuxe K. Neurosci Lett. 1997; 239:61–64. [PubMed: 9469656]
50. Levant B, Grigoriadis DE, DeSouza EB. J Pharmacol Exp Ther. 1992; 262:929–935. [PubMed: 1356154]
51. Ewing AG, Dayton MA, Wightman RM. Anal Chem. 1981; 53:1842–1847.
52. Vreeland RF, Atcherley CW, Russell WS, Xie JY, Lu D, Laude ND, Porreca F, Heien ML. Anal Chem. 2015; 87:2600–2607. [PubMed: 25692657]
53. Nimitvilai S, Brodie MS. J Pharmacol Exp Ther. 2010; 333:555–563. [PubMed: 20164301]
54. Van Muiswinkel FL, Drukarch B, Steinbusch HWM, Stoof JC. Exp Neurol. 1994; 125:218–227. [PubMed: 7906226]
55. Drukarch B, Schepens E, Stoof JC. Eur J Pharmacol. 1991; 196:209–212. [PubMed: 1678719]

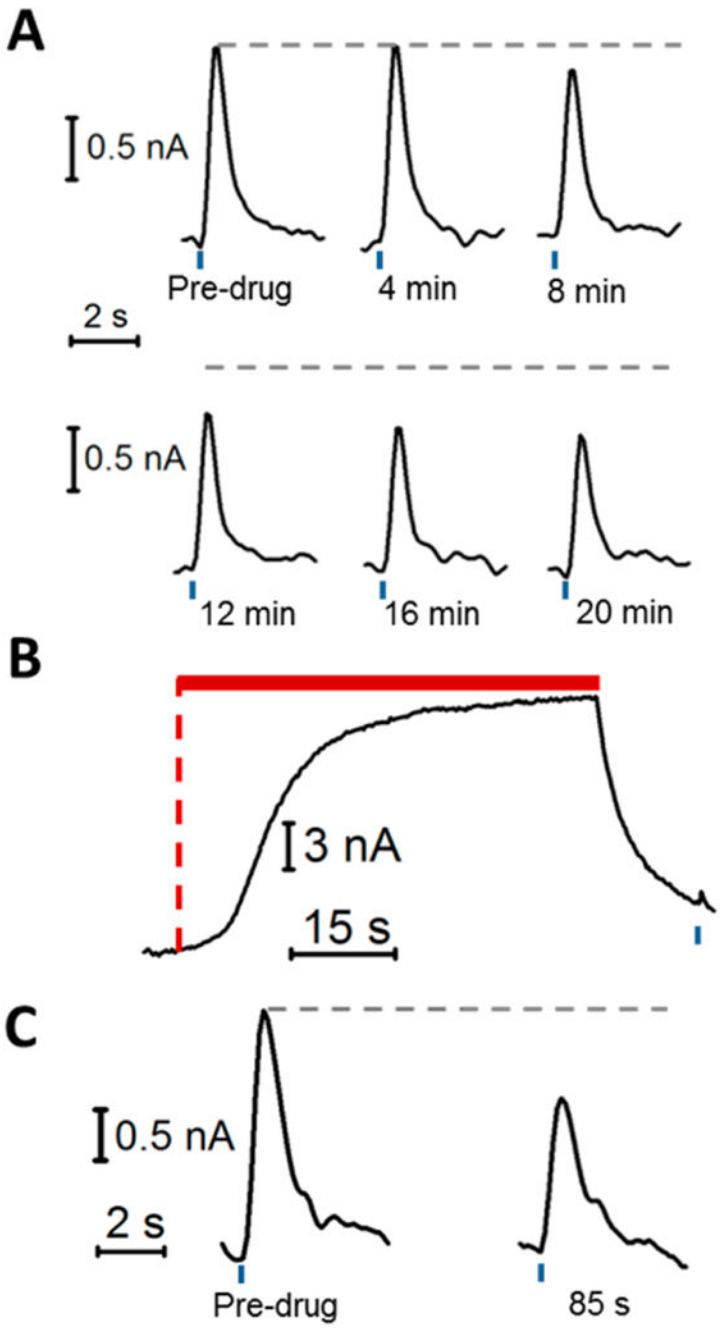

Figure 1.

Comparison of drug administration by perfusion and controlled iontophoresis in the dorsal striatum of a brain slice. (A) Electrically evoked DA release was monitored with a microelectrode during perfusion of 30 nM QP. The released amount before drug (termed predrug, dashed gray line) was established, and the perfusion stream was switched to aCSF containing QP; this time was taken as $t = 0$. Stimulation continued every 4 min (blue bars) until the new release quantity was stable. (B) Controlled iontophoretic delivery of QP. An iontophoretic probe containing a carbon-fiber microelectrode was used to eject a solution of

QP, DHBA, and NaCl (0.4, 0.2, 5 mM, respectively) at 15 nA for 60 s (red bar). The oxidation of DHBA upon ejection was detected by FSCV performed on the electrode. DA release was elicited 15 s after the end of the ejection and was also detected by the carbon fiber. (C) Comparison of pre- and postdrug DA release following the ejection in (B).

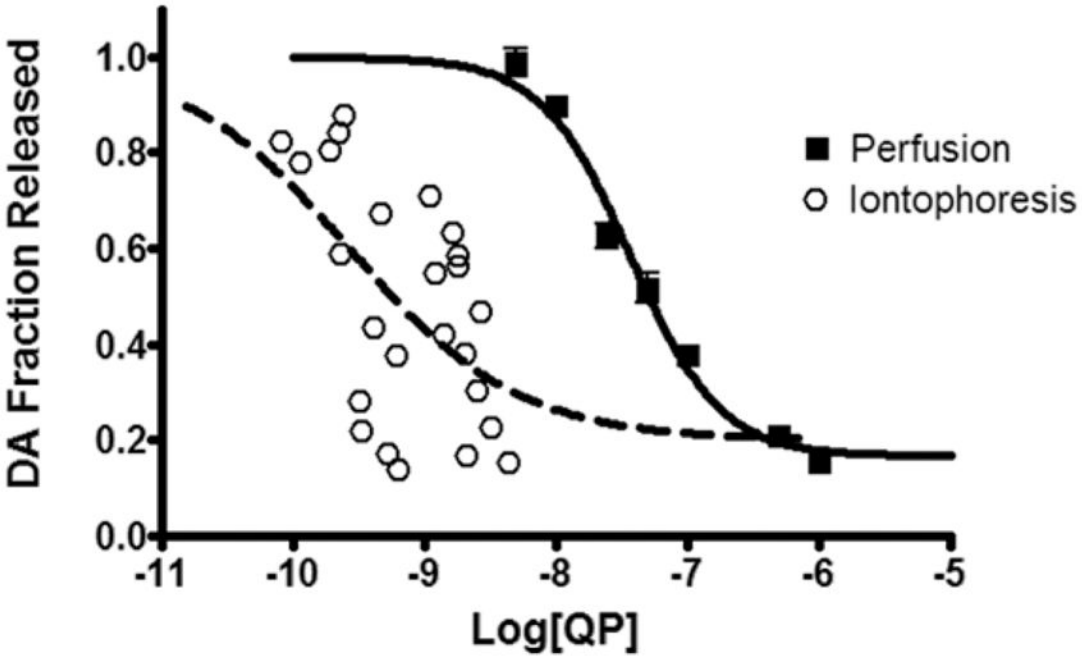

Figure 2.

Dose–response data for the effect of QP on stimulated DA release in the dorsal striatum. QP was delivered by perfusion (squares, $n = 5$ per concentration) or controlled iontophoresis (circles). Iontophoretic ejections (5 ejections from 5 unique probes) were monitored using AP, and QP concentrations were evaluated using eq 1. Error bars for perfusion represent the SEM.

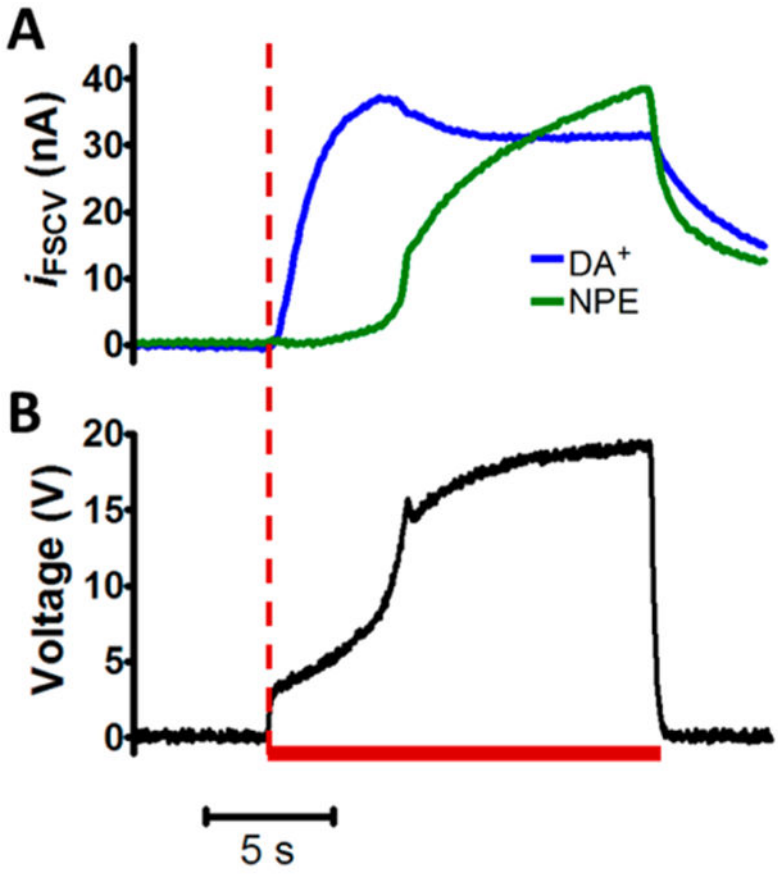

Figure 3.

Combined delivery of differently charged species. (A) Faradaic current versus time traces for DA (blue) and NPE (green) during coejection. A solution of 1 mM DA, 11 mM NPE, and 5 mM NaCl was ejected (red bar) into aCSF while a carbon-fiber microelectrode was used to monitor delivery. (B) Ejection voltage required to supply 30 nA for the ejection in (A).

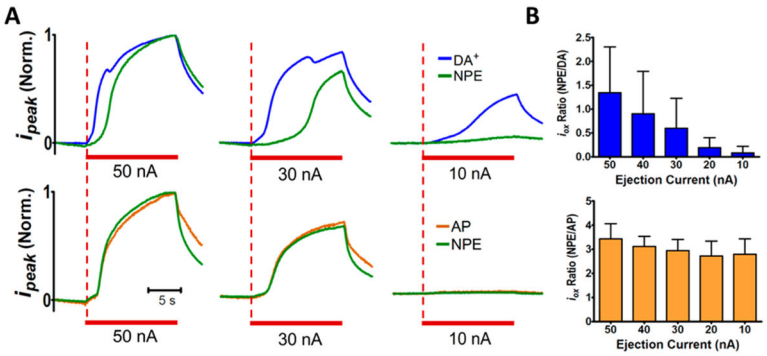

Figure 4.

Variation in delivery profiles of coejected species with ejection current. (A) Representative current versus time traces for coejected species when ejected using different currents. Delivery from barrels containing 1 mM DA (blue) and 11 mM NPE (green) reveal differential ejection amounts with the ejection current magnitude (upper). Solutions of 5 mM AP (orange) and 11 mM NPE (green) resulted in similar delivery profiles (lower). All profiles were normalized to the maximum value obtained during the 50 nA ejection. Solutions also contained 5 mM NaCl. (B) Ratio of the maximum faradaic current of coejected species for NPE/DA (upper) and NPE/AP (lower).

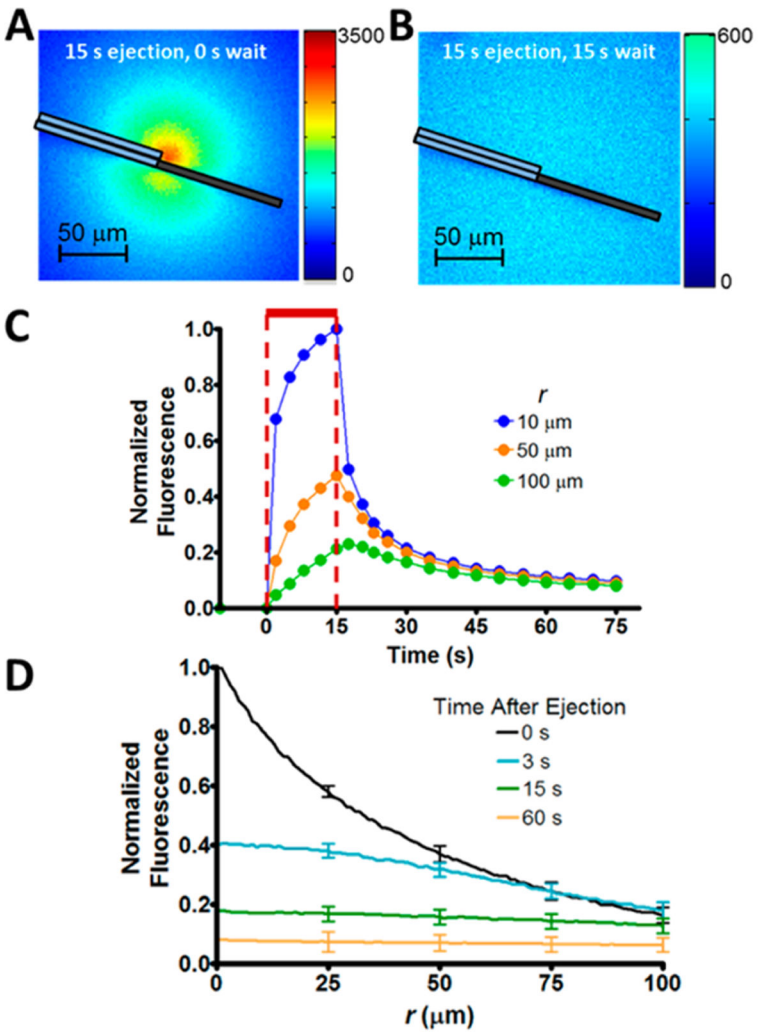

Figure 5.

Distribution of ejected solute during and after iontophoretic delivery. (A) Color plot of $Ru(bpy)_3^{2+}$ fluorescence intensity at the end of a 15 s ejection and (B) the same distribution after a 15 s waiting period during which the ejection current was disabled. The location of the carbon-fiber electrode (black) and iontophoretic barrel (light blue) are indicated by the overlaid representation. (C) Fluorescence intensity on a sphere of radius *r* centered at the ejection origin during and following ejection ($n = 8$). All values were normalized to the maximum intensity 10 μm from the ejection point. The red bar represents the ejection time, and the dashed vertical lines indicate its initiation and termination. (C) Distribution of ejected solute along the length of the carbon-fiber electrode at select time points following a 15 s iontophoretic delivery.

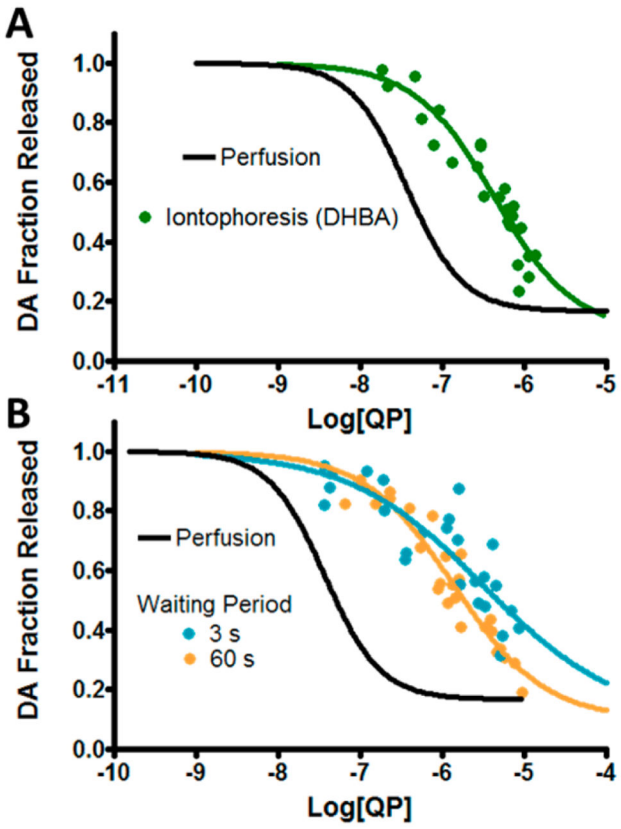

Figure 6.

Controlled iontophoretic dose–response data for QP administration using DHBA to monitor ejections. (A) Responses following 15 s ejections with a 15 s waiting period. (B) Dose–response data for 3 and 60 s waiting periods following 15 s ejections. For all ejections, eq 1 was used to evaluate concentrations using the fluorescence dilution factor (DF = 0.94, 0.55, and 0.25 for the 3, 15, and 60 s waiting periods, respectively). Barrels contained 0.2 mM DHBA and 0.05 mM QP for the 3 and 15 s waiting periods. For 60 s, this was increased to 0.4 mM DHBA and 0.2 mM QP. All barrels contained 5 mM NaCl, and each data set is comprised of 5 ejections from 5 unique probes.

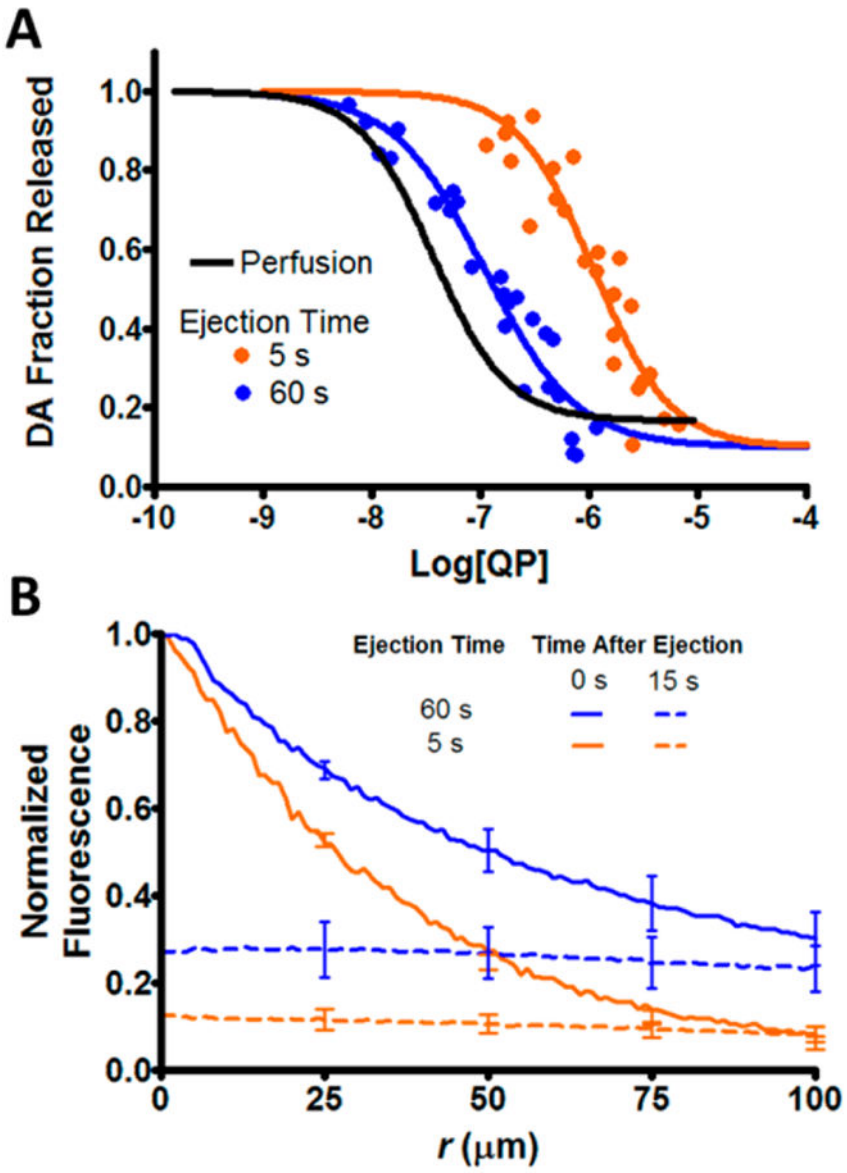

Figure 7.

Ejection length increases accuracy of concentration evaluations. (A) Dose–response data for 5 and 60 s controlled iontophoretic ejections with a 15 s waiting period. Ejections were monitored using DHBA, and eq 1 was used to evaluate ejection concentrations (DF was 0.63 and 0.62 for 5 and 60 s ejection periods, respectively). Barrels performing 5 s ejections contained 0.4 mM DHBA and 0.1 mM QP in 5 mM NaCl, which was changed to 0.2 mM DHBA and 0.0125 mM QP in 10 mM NaCl for 60 s ejections. Each data set includes 5 ejections from 5 unique probes. (B) Solute distribution following ejections and a 15 s waiting period. Ejections of Ru(bpy)32+ were performed into agarose for 5 and 60 s ($n = 8$). For each case, the fluorescence was normalized to the maximum value at the end of the ejection.

Table 1

Parameters of Perfusion and Iontophoretic Dose-Response Data for QP Administration and Its Effect on Stimulated DA Release[a]

	perfusion	iontophoresis
log(IC_{50})	−7.43 ± 0.04	−9.57 ± 0.83
Hill slope	−1.28 ± 0.12	−0.68 ± 0.83
r^2	0.966	0.296

[a]Parameters are from analysis of data shown in Figure 2 using a four parameter Hill model. Perfusion trials utilized 5 measurements at each concentration. Iontophoretic data was obtained by 5 ejections from 5 different probes. AP was used as the electrochemical marker, and concentrations were evaluated using eq 1. Entries indicate the value and SEM.

Table 2

Parameters of Iontophoretic Dose-Response Data for QP Administration on Stimulated DA Release Following Different Waiting Periods[a]

	3 s	15 s	60 s
log(IC_{50})	−5.32 ± 0.99	−6.25 ± 0.42	−5.72 ± 0.31
Hill slope	−0.51 ± 0.26	−0.83 ± 0.24	−0.71 ± 0.16
r^2	0.723	0.887	0.906

[a]The time indicates the duration between the end of the ejection and DA stimulation. Parameters reflect data displayed in Figure 6A,B, which were obtained by 5 ejections from 5 different probes. DHBA was used to monitor ejections, and concentrations were evaluated using eq 1 with the updated fluorescence DF method. A four parameter Hill model was used to evaluate parameters, and entries indicate the value and SEM.

Table 3

Parameters of Iontophoretic Dose-Response Data for QP Administration on Stimulated DA Release Following Different Ejection Durations[a]

	3 s	15 s
log(IC_{50})	−5.96 ± 0.14	−6.84 ± 0.15
Hill slope	−1.25 ± 0.27	−0.90 ± 0.16
r^2	0.876	0.941

[a]The time indicates the ejection duration, which was followed with a 15 s waiting period before DA stimulation. Parameters represent data in Figure 7A, obtained by 5 ejections from 5 different probes. Concentrations were evaluated from eq 1 using the DHBA marker current and updated DF term.